

# Experimental demonstration of two methods for controlling the group delay in a system with photonic-crystal resonators coupled to a waveguide

Yijie Huo,<sup>1,5,†</sup> Sunil Sandhu,<sup>1,†</sup> Jun Pan,<sup>2,†</sup> Norbert Stuhmann,<sup>1</sup> Michelle L. Povinelli,<sup>3</sup>  
Joseph M. Kahn,<sup>1</sup> James S. Harris,<sup>1</sup> Martin M. Fejer,<sup>4</sup> and Shanhui Fan<sup>1,6</sup>

<sup>1</sup>Department of Electrical Engineering, Stanford University, Stanford, California 94305, USA

<sup>2</sup>Department of Materials Science and Engineering, Stanford University, Stanford, California 94305, USA

<sup>3</sup>Ming Hsieh Department of Electrical Engineering, University of Southern California, Los Angeles, California 90089, USA

<sup>4</sup>Department of Applied Physics, Stanford University, Stanford, California 94305, USA

<sup>5</sup>e-mail: yjhuo@stanford.edu

<sup>6</sup>e-mail: shanhui@stanford.edu

Received February 24, 2011; accepted February 26, 2011;  
posted March 21, 2011 (Doc. ID 142938); published April 15, 2011

We measure the group delay in an on-chip photonic-crystal device with two resonators side coupled to a waveguide. We demonstrate that such a group delay can be controlled by tuning either the propagation phase of the waveguide or the frequency of the resonators. © 2011 Optical Society of America

OCIS codes: 130.3120, 230.5298, 230.4555, 200.4490.

There has been substantial recent interest in mapping coherent effects of atomic systems into on-chip microresonator systems [1–7]. Whereas the coherent effects in atomic systems occur due to the quantum interference induced by coherently driving the atom with an external laser, the coherent interference between coupled resonators is enforced by the geometry of the nanophotonic structure. As compared to atomic systems, these microresonator systems are compatible with on-chip integration and room-temperature operation and are tunable over a wide optical communication wavelength range. In particular, there have been significant developments in demonstrating the all-optical analogue to electromagnetically induced transparency (EIT). In EIT, the narrow transparency peak in the transmission spectrum is associated with a large group delay, which has been experimentally measured in a two-microresonator system [8]. As a static system, such a two-microresonator system is fundamentally limited by the delay–bandwidth product constraint—the maximum achievable delay is inversely proportional to the operating bandwidth [9]. On the other hand, in an EIT-like system, there is an opportunity to overcome such a delay–bandwidth product constraint by dynamic tuning [10]. Therefore, fully characterizing the group delay spectrum, as well as demonstrating the control of such a group delay, is an important step forward in developing dynamic photonic systems.

In this Letter, we experimentally demonstrate the control of the group delay in a photonic-crystal (PC) device consisting of two microresonators side coupled to a waveguide (Fig. 1). We demonstrate a tuning of the group delay between 5 and 16 ps in this device. When the peak delay is 16 ps, the delay of the device is above 8 ps over a bandwidth of 20 GHz. In particular, we demonstrate that the group delay in this device can be controlled by tuning either the propagation phase of the waveguide or the frequency of the resonators.

A scanning electron microscope (SEM) image of the top view of our PC structure is shown in Fig. 1(a).

The system consists of two resonators side coupled to an optical PC waveguide. The center-to-center separation of the resonators was  $L = 140a$ , where  $a = 386$  nm was the nearest-neighbor hole separation (lattice constant). Details on the fabrication process are given in Ref. [6]. When properly designed, the system can exhibit an EIT-like transmission spectrum, as discussed in Ref. [11].

Figure 2 shows the experimental setup used to measure the group delay of our PC device [Fig. 1] by the modulation phase shift method. A cw signal from a tunable laser source is directed into a component analyzer, which performs electro-optic modulation of its intensity at a frequency  $\omega_m/2\pi$ . The modulation frequency is swept from 0.05 to 5 GHz. Spectral broadening due to this modulation is small compared to the device EIT spectral features. The modulated light's TE component is focused into the inverse taper of the silicon strip waveguide. At the output of the PC device, light is collected by a lensed single-mode fiber, and 10% of this collected power is directed

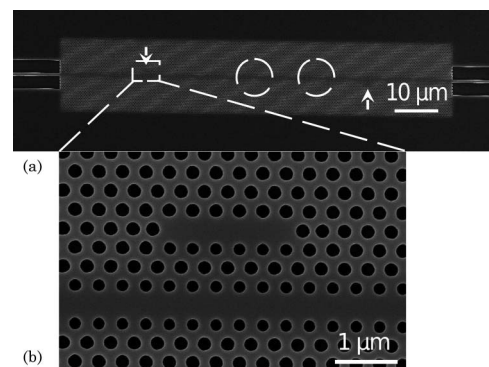


Fig. 1. SEM images of the fabricated device. (a) Top view of the photonic-crystal structure with two resonators (indicated by arrows) side coupled to a waveguide, (b) magnified view of the region around the left PC resonator. The tuning laser position is also indicated by dashed white circles for both the EIT-like (left circle) and far detuned (right circle) cases.

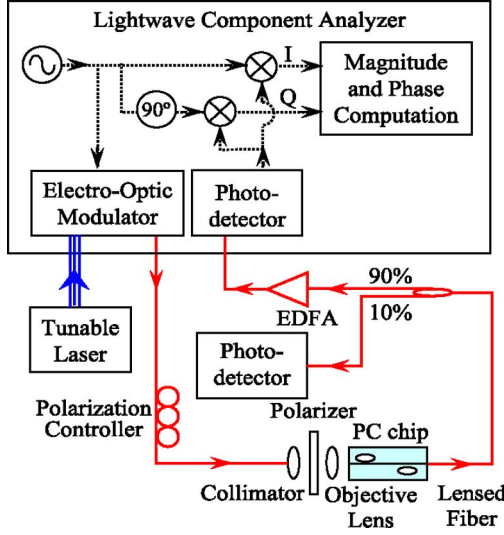


Fig. 2. (Color online) Optical time-delay measurement setup. The dotted black lines, triple blue lines, and single red line represent the RF coaxial cables, polarization-maintaining fibers, and single-mode fibers, respectively.

onto a calibrated Ge photodetector for transmission amplitude measurements. The remaining 90% of the collected power is amplified by an L-band erbium-doped fiber amplifier (EDFA) and directed to the input of the component analyzer, which measures both the in-phase  $i_I$  and quadrature  $i_Q$  components of the photocurrent generated by the detected signal at a frequency  $\omega_m$ . From the phase shift  $\Phi(\omega, \omega_m) = \tan^{-1}(i_Q/i_I) = \omega_m \tau_{GD}(\omega)$ , the group delay  $\tau_{GD}(\omega) = \partial\Phi/\partial\omega_m$  of the PC device can be determined with an accuracy of about 1 ps, as limited by the noise level of the optical detector.

Controlling of the device's group delay is carried out thermo-optically by either tuning the propagation phase of the waveguide or detuning the PC resonators' resonant frequencies, using a 532 nm green laser focused to a 10  $\mu\text{m}$  diameter spot size on the PC device [11].

Figure 3 shows the transmission and relative group delay spectra for three different tuning conditions. Prior to any temperature tuning, the detuning between the two resonators is 0.35 nm. In Figs. 3(a)–3(d), we focus the laser spot close to the center of the whole device in order to dynamically tune the propagation phase in the waveguide. In the case of Figs. 3(a) and 3(b), the system's round-trip phase is  $\sim 2n\pi$  (where  $n$  is an integer) resulting in an EIT-like transmission spectrum [Fig. 3(a)]. The corresponding measured relative group delay [Fig. 3(b)] has a maximum value of 16 ps around the EIT-like transparency peak. This value exceeds the sum of delays from the waveguide and the resonators by a factor of 4. Having such excess delay indicates that the resonators do interfere and, therefore, that the physics here is different from the resonator system in Ref. [12]. In Figs. 3(c) and 3(d), the round-trip phase is tuned away from  $2n\pi$ , resulting in a more asymmetric transmission spectrum [Fig. 3(c)] with a maximum relative group delay value of 12 ps [Fig. 3(d)]. We next dynamically detune the resonant frequency difference between the PC resonators to  $> 1$  nm by aiming the laser spot closer to one of the resonators

(Fig. 1). In this far detuned case, the maximum relative group delay is 5 ps [Fig. 3(f)].

The experimental transmission and group delay spectra in Fig. 3 are well described using coupled mode theory [4]. The field transmission of the system can be written as

$$t(\omega) = \frac{t_A(\omega)t_B(\omega) \exp[j\beta(\omega)L]}{1 - r_A(\omega)r_B(\omega) \exp[j2\beta(\omega)L]}, \quad (1)$$

where  $t_{A,B}$  and  $r_{A,B}$  are the transmission and reflection coefficients, respectively, for resonator  $A$  or  $B$ , given by the following equations:

$$t_{A,B}(\omega) = \frac{j(\omega - \omega_{A,B}) - \gamma_{A,B}}{j(\omega - \omega_{A,B}) - (\gamma_{cA,B} + \gamma_{A,B})}, \quad (2)$$

$$r_{A,B}(\omega) = \frac{\gamma_{cA,B}}{j(\omega - \omega_{A,B}) - (\gamma_{cA,B} + \gamma_{A,B})}, \quad (3)$$

where  $\omega_{A,B}$  is the resonant frequency of resonator  $A$  or  $B$ .  $\gamma_{A,B}$  is its amplitude intrinsic loss rate, related to the intrinsic quality factor  $Q_{\text{int}A,B}$  as  $\gamma_{A,B} = \omega_{A,B}/2Q_{\text{int}A,B}$ , and  $\gamma_{cA,B}$  is the amplitude resonator–waveguide coupling rate, related to the coupling quality factor  $Q_{cA,B}$  as  $\gamma_{cA,B} = \omega_{A,B}/2Q_{cA,B}$ . From Eq. (1), the system group delay is

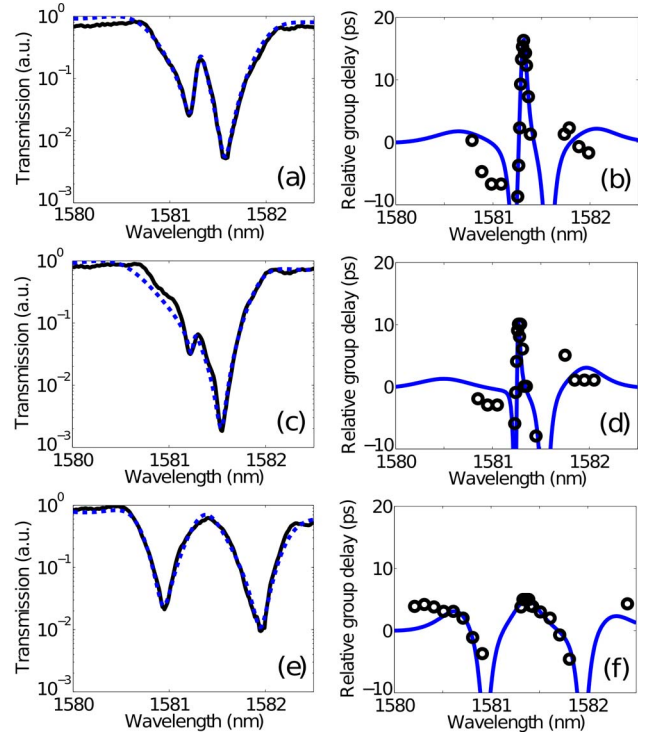


Fig. 3. (Color online) Transmission spectrum (left) and relative group delay spectrum (right) of the PC device for three different tuning conditions. (a), (c), (e) Experimental data (solid black line) and the theoretical fits (dashed blue line) of the transmission spectrum, (b), (d), (f) experimental data (circles) and the theoretical fit (solid blue line) of the relative group delay spectrum.

$$\tau_{\text{GD}}(\omega) = \frac{d\text{Arg}[t(\omega)]}{d\omega} = \frac{|r_A(\omega)r_B(\omega)|\tau_{\text{GD,RT}}(\omega)(|r_A(\omega)r_B(\omega)| - \cos[\theta(\omega)]) - \frac{d|r_A(\omega)r_B(\omega)|}{d\omega}\sin[\theta(\omega)]}{-|r_A(\omega)r_B(\omega)|^2 - 1 + 2|r_A(\omega)r_B(\omega)|\cos[\theta(\omega)]} + \tau_{\text{GD,DP}}(\omega), \quad (4)$$

where  $\theta(\omega) = \text{Arg}[r_A(\omega)] + \text{Arg}[r_B(\omega)] + 2\beta(\omega)L$  is the round-trip phase in the system,  $\tau_{\text{GD,RT}}(\omega) = d\theta(\omega)/d\omega$  is the round-trip group delay in the system, and  $\tau_{\text{GD,DP}}(\omega) = d\text{Arg}[t_A(\omega)]/d\omega + d\text{Arg}[t_B(\omega)]/d\omega + Ld\beta(\omega)/d\omega$  is the “direct-path” group delay through the system. The system relative group delay is obtained from Eq. (4) as follows:

$$\Delta\tau_{\text{GD}}(\omega) = \tau_{\text{GD}}(\omega) - \tau'_{\text{GD,DP}}, \quad (5)$$

where  $\tau'_{\text{GD,DP}} = \tau_{\text{GD,DP}}(\omega)$  is the constant system group delay value in the frequency region far away from the resonators' resonances where the reflections  $r_A$  and  $r_B$  in Eq. (4) are 0.

At the peak of the EIT-like transmission spectrum, the round-trip phase  $\theta(\omega_0)$  is  $2n\pi$  and the system group delay [Eq. (4)] becomes  $\tau_{\text{GD}}(\omega_0) = \tau_{\text{GD,RT}}\xi + \tau_{\text{GD,DP}}$ , where  $\xi = |r_A r_B|/(1 - |r_A r_B|)$ . In this system, the *dark state* (i.e., the high- $Q$  resonance) is the Fabry–Perot resonance between the resonators, while the low- $Q$  resonances are the resonators themselves. The coupling between them gives rise to the EIT-like effect.

The dashed and solid blue lines in Fig. 3 show the theoretical fits for the transmission spectrum [Eq. (1)] and relative group delay spectrum [Eqs. (4) and (5)]. In the plots, the dispersion for the waveguide was obtained from direct numerical simulation of the waveguide:  $\beta(\omega) = 5.6 \times 10^{-8} \text{ m}^{-1} \text{ s } \omega - 7.3 \times 10^7 \text{ m}^{-1}$ . The resonance frequencies  $\omega_A$  and  $\omega_B$  were found from the minima in the transmission spectra, and the remaining parameters were fitted using the transmission spectra in the following manner.  $Q_{\text{CA,B}}$  was adjusted between 1600 and 4700 to fit the background wide transmission dip, and  $Q_{\text{intA,B}}$  was adjusted between 11,000 and 32,000 to fit the amplitude of the central peak. The waveguide length was adjusted between  $54.04 \mu\text{m}$  and  $54.14 \mu\text{m}$  to fit the shape of the central peak. These adjustments in the parameters between the plots in Fig. 3 are due to the effects of the thermo-optical tuning of the propagation phase of the waveguide and the PC resonators' resonant frequencies that were performed in the experiments.

In the case of Fig. 3(b), the relative group delay of the system is enhanced by the first term in Eq. (4) for the wavelength region where there are multiple constructively interfering reflections between the resonators (i.e., round-trip phase  $\theta(\omega) \approx 2n\pi$ ), and the measured maximum relative group delay exceeds the minimum group delay of the system [ $\tau_{\text{GD,DP}}$  in Eq. (4)] by a factor of 4. As for the far detuned case of Fig. 3(f), there is very little coherent interaction between resonators for all wavelengths, and the group delay of the system is mainly due to the direct-path delay,  $\tau_{\text{GD,DP}}(\omega)$ .

In conclusion, we have experimentally demonstrated two methods of controlling the group delay in an on-chip PC resonator system. By dynamically tuning the propagation phase of the waveguide, we demonstrated relative group delay control between 12 ps and 16 ps. Alternatively, by dynamically tuning the resonant frequencies of the PC resonators, we were able to control the relative group delay between 5 ps and 16 ps. Our work on the above two ways of controlling the group delay is an important step toward the realization of a dynamic light trapping system [10]. Although the thermo-optical tuning method used in our experiments can only have modulation rates of up to  $\sim 1$  MHz, faster modulation rates, greater than 20 GHz, can be achieved using the fully integrated carrier injection/removal tuning methods discussed in Refs. [13,14].

This work was supported in part by the Slow Light program at the Defense Advanced Research Projects Agency (DARPA) Defense Sciences Office, under the Air Force Office of Scientific Research AFOSR Grant No. FA9550-05-0414.

\*These authors contributed equally to this work.

## References

1. E. Arimondo and G. Orriols, *Lett. Nuovo Cimento* **17**, 333 (1976).
2. S. E. Harris, *Phys. Today* **50** (7), 36 (1997).
3. R. H. Dicke, *Phys. Rev.* **93**, 99 (1954).
4. Q. Xu, S. Sandhu, M. L. Povinelli, J. Shakya, S. Fan, and M. Lipson, *Phys. Rev. Lett.* **96**, 123901 (2006).
5. X. Yang, M. Yu, D.-L. Kwong, and C. W. Wong, *Phys. Rev. Lett.* **102**, 173902 (2009).
6. J. Pan, S. Sandhu, Y. Huo, N. Stuhmann, M. L. Povinelli, J. S. Harris, M. M. Fejer, and S. Fan, *Phys. Rev. B* **81**, 041101 (2010).
7. J. B. Khurgin, D. Yang, and Y. J. Ding, *J. Opt. Soc. Am. B* **18**, 340 (2001).
8. Q. Xu, J. Shakya, and M. Lipson, *Opt. Express* **14**, 6463 (2006).
9. G. Lenz, B. J. Eggleton, C. K. Madsen, and R. E. Slusher, *IEEE J. Quantum Electron.* **37**, 525 (2001).
10. M. F. Yanik, W. Suh, Z. Wang, and S. Fan, *Phys. Rev. Lett.* **93**, 233903 (2004).
11. J. Pan, Y. Huo, S. Sandhu, N. Stuhmann, M. L. Povinelli, J. S. Harris, M. M. Fejer, and S. Fan, *Appl. Phys. Lett.* **97**, 101102 (2010).
12. J. Cardenas, M. A. Foster, N. Sherwood-Droz, C. B. Poitras, H. L. R. Lira, B. Zhang, A. L. Gaeta, J. B. Khurgin, P. Morton, and M. Lipson, *Opt. Express* **18**, 26525 (2010).
13. Q. Xu, B. Schmidt, S. Pradhan, and M. Lipson, *Nature* **435**, 325 (2005).
14. T. Tanabe, E. Kuramochi, H. Taniyama, and M. Notomi, *Opt. Lett.* **35**, 3895 (2010).